Electronic and vibrational density of states through the metal-insulator transition in amorphous yttrium-silicon alloy thin films

B. L. Zink[*]

Department of Physics and Astronomy, University of Denver, Denver, Colorado 80208-6900, USA

F. Hellman

Department of Physics, University of California, Berkeley, California 94720-7300, USA

We present specific-heat measurements from 3–100 K of amorphous yttrium-silicon alloy films with compositions spanning the metal-insulator transition. In samples near or above the metal-insulator transition, we observe an electronic contribution to specific heat. Comparison to undoped amorphous silicon grown by the same technique allows a quantitative analysis of the vibrational modes associated with the heavy dopant atoms. The dopant atoms add nonpropagating vibrational modes to the amorphous-silicon matrix that can be modeled with Einstein modes. Near metal-insulator transition, an additional contribution to specific heat appears that is most pronounced on the metallic side. We explore two possible explanations for this excess heat capacity: a significant change in the vibrational modes or an origin related to the correlated-electron physics of the metal-insulator transition.

PACS number(s): 65.60.+a, 61.43.Dq, 63.50.−x, 71.30.+h

I. INTRODUCTION

Two of the most important themes of recent research across condensed-matter physics are disorder and the consequences of electron interactions. These two concepts dominate the study of the disorder- and Coulomb interaction-driven metal-insulator transition (MIT).[1] As suggested by Anderson, in a disordered electronic system the randomization of the phase of the electron wave functions causes the states with energy below the mobility edge to be localized within a localization length ξ, which can be much greater than the interatomic spacing.[2] The Fermi energy E_F can be changed by adding atoms that either donate or accept electrons. When $E_F < E_c$, ξ is finite, conductivity is zero at $T=0$, and conduction can occur only by thermally activated hopping of electrons from one localized state to another. When $E_F > E_c$, ξ diverges and the resulting extended states allow metallic conduction. Therefore in this disordered single-electron picture, in theory the transition from insulator to metal occurs when E_F moves through E_c as the electronic content of the material is increased.

Electron-electron interactions cause a gap in the single-electron density of states (DOS) centered around the Fermi energy that substantially modifies conductivity near the metal-insulator transition and typically dominates the MIT physics of disordered or amorphous systems. In materials such as amorphous niobium silicon, a-Nb$_x$Si$_{1-x}$, as well as in boron-doped silicon, Si:B, the single-particle electron density of states, $g(E)$, near the Fermi energy has been directly measured by tunneling spectroscopy.[3,4] These experiments confirm that $g(E_F)=0$ in the insulating state, due to the formation of this Coulomb gap, and that the MIT is driven by a combination of disorder and correlation effects.

Low-temperature specific-heat measurements measure the low-lying excitations of a system. In a simple metal, this gives the electron density of states at the Fermi energy, which is proportional to the electronic specific-heat coefficient γ. In contrast to tunneling spectroscopy, this γ does not exclusively measure single-particle states but includes contributions from many-body excitations, which are often invoked when experiments on systems expected to give zero electronic DOS result in finite values of γ. For example, low-temperature specific-heat studies of crystalline bulk Si:P near the MIT indicate a finite, smoothly varying γ through the transition, but a rapid reduction near the transition on the insulating side.[5,6] The phonon contribution is well described by the Debye function $C_{phon}=\beta T^3$ at low T, and an excess specific heat proportional to T^α, with $\alpha \sim 0.2$, appears that is due to magnetic moments in this seemingly nonmagnetic system. The presence of magnetic moments is confirmed by magnetic-susceptibility measurements[7–9] and occurs because Coulomb interactions cause electrons in localized states to prefer single occupation over the double occupation suggested by the Pauli principle. These unpaired localized electrons constitute local magnetic moments, which interact via exchange and give a nontrivial contribution to specific heat and magnetic susceptibility. Application of a magnetic field to this system causes dramatic changes in this excess specific heat as the previously degenerate magnetic states split into two level systems causing Schottky contributions to the specific heat. These effects primarily occur at $T < 1$ K for crystalline systems but could theoretically be seen at higher temperatures in amorphous systems due to the much larger electron concentration at the MIT.[10] These many-body interactions can also lead to time-dependent electronic properties, including the electronic specific heat, though a time-dependent specific heat has not been observed experimentally to our knowledge.[11,12]

Previously reported specific-heat measurements on the transition-metal-doped amorphous semiconductors, which include a-Mo$_x$Ge$_{1-x}$,[13] a-Ti$_x$Si$_{1-x}$,[14,15] a-V$_x$Si$_{1-x}$,[16] and a-Au$_x$Si$_{1-x}$,[17] also indicate finite values of γ. The metal-insulator transition in these materials is the same as in Si:P in most respects, with the most substantive differences arising

from the large electron concentrations (10^{22} cm^{-3}). These studies focus almost exclusively on specific heat between 1 and 10 K and generally give a simpler picture of the specific heat near the transition, with the a-V$_x$Si$_{1-x}$ and a-Ti$_x$Si$_{1-x}$ well described by

$$C = \gamma T + \beta T^3, \tag{1}$$

with γ between 0.5 and 1 mJ/mol K^2 near the transition.[15,16] a-Mo$_x$Ge$_{1-x}$ shows an additional δT^5 contribution and an excess specific heat on the insulating side and has somewhat smaller γ.[13] In all these materials, γ varies smoothly through the MIT, with no apparent sharp reduction on the insulating side. These materials have also not been previously studied at higher temperatures, where amorphous solids almost always have a well-defined broad maximum in C/T^3, typically seen near 10–20 K.[18,19] This large bump in C/T^3 is due to excess vibrational modes associated with the amorphous structure. Along with these excess modes, amorphous insulators almost always also have a linear term in the specific heat at temperatures <1 K on the order 5×10^{-5} J/mol K^2 (significantly smaller than the linear terms seen in disordered electronic systems), which is attributed to a constant density of two-level state (TLS) systems at low energies in the vibrational spectrum rather than electronic or magnetic states.[20,21] It is still a matter of debate whether these phenomena can be explained in a single theoretical framework. Interestingly, both theory and various experimental techniques including specific heat have proven that amorphous silicon has both fewer of these presumably structural TLS excitations and a smaller peak in C/T^3 than typical glasses, which is likely due to the overconstrained fourfold covalent bonds.[20,22–26] It is still unknown how the addition of dopants such as Y, Nb, V, or Ti affects these phenomena.

In this paper, we report specific heat of a-Y$_x$Si$_{1-x}$ films measured using a Si-N membrane-based microcalorimeter[27,28] from 3–100 K, a wider temperature range than previously measured for any nonmagnetic-doped amorphous semiconductor. This system is very similar to the well-studied a-Nb$_x$Si$_{1-x}$, with the transition occurring near $x=0.14$, and an electron concentration that is large relative to Si:P. Estimates of the electron concentration range from $\sim 3 \times 10^{20}$ cm^{-3} from optical absorption to $\sim 5 \times 10^{22}$ cm^{-3} from assuming $3e^-$ are donated by each trivalent Y^{3+}.

Recent investigations have begun to shed some light on the local atomic structure of this alloy, as well as the vibrational density of states (VDOS). Meregalli and Parrinello performed local density-functional theory calculations for a-Y$_x$Si$_{1-x}$, which indicate that Y^{3+} ions are surrounded by under-coordinated Si, forming a cage of dangling bonds.[29] They also associated two features in the calculated VDOS with Y doping, a shoulder at 70 cm^{-1} (8.7 meV), and a peak at 180 cm^{-1} (22 meV) that they attributed to the dangling bonds. X-ray fine-structure (XAFS) measurements of the structurally analogous a-Gd$_x$Si$_{1-x}$ also indicate that the metal dopants are surrounded by Si atoms but do not support the presence of dangling bonds.[30] We have also reported thermal conductivity and specific heat of a-Si,[25] as well as C for a a-Y$_{0.09}$Si$_{0.91}$ sample and k for several doped a-Si thin films.[31] Addition of Y to the a-Si matrix significantly reduces the

thermal conductivity while apparently adding excess vibrational modes to the specific heat. Here, we present a more detailed study of the specific heat of a-Y$_x$Si$_{1-x}$ for a range of x. We use the results to probe the vibrational, electronic, and correlated-electron behaviors near the MIT in an amorphous thin-film system with strong disorder.

II. EXPERIMENTAL DETAILS

The microcalorimeter measurements begin by thermally evaporating an ≈ 2000 Å Al thermal-conduction layer onto the central area of the calorimeter's 2000-Å-thick silicon-nitride-membrane sample platform. This film keeps the membrane heater, thermometers, and sample isothermal. Onto this Al underlayer, we electron-beam (e-beam) co-evaporate 3500–4000-Å-thick a-Y$_x$Si$_{1-x}$ films with $0.09 < x < 0.21$ in a UHV system at $\leq 10^{-8}$ Torr. Y and Si are evaporated from separate sources, and the temperature of the sample holder is monitored and stays below 80 °C during the deposition. Samples are also deposited on Si-N-coated Si substrates which are used for profilometry to measure the film composition and areal density of atoms by Rutherford backscattering (RBS) and for structural characterization. X-ray diffraction, transmission electron microscopy (TEM),[31] and XAFS (Ref. 30) confirm the amorphous structure of the films with no observable clustering of Y atoms or formation of voids. Transmission electron microscopy of similar samples confirm the amorphous structure with excellent homogeneity up to $x \sim 0.25$.[32] The background or addenda heat capacity is approximately 66% of the total at low T and 50% of the total at 100 K. The error on each measurement is $\approx 2\%$, giving errors on the sample specific heat of between 9% and 15% at 4 K and 5% and 6% at higher T. Further details of the microcalorimetry techniques, including typical values of addenda heat capacity as a function of T, are given elsewhere.[27,28]

III. RESULTS

Figure 1 presents the specific-heat data on a traditional C/T vs T^2 plot for four a-Y$_x$Si$_{1-x}$ films, as well as an amorphous-silicon film ($x=0$) grown with the same techniques and described in detail elsewhere.[25] Here and in all other plots, we use molar units (i.e., J/mol K) where the mole counts both Y and Si atoms. A specific heat of the type $C=\gamma T+\beta T^3$ is a straight line on this plot, with the y intercept indicating the electronic specific-heat coefficient γ. Even over the rather small temperature range shown in Fig. 1, C/T for Y-doped films shows curvature. This is the first indication that the specific heat is not well described by a simple Debye function at these temperatures. Note that the solid lines shown in Fig. 1 result from the fit described below and are not simply $\gamma T+\beta T^3$. It is common to determine γ from a simple linear fit of the data plotted as shown in Fig. 1. When the vibrational contributions to C are clearly Debye-like and no other significant excitations are present, this is a straight-forward and reliable procedure.

As shown in Fig. 2, this is not the case in the doped a-Si alloys. Here we plot C/T^3 vs T for the same a-Y$_x$Si$_{1-x}$ films
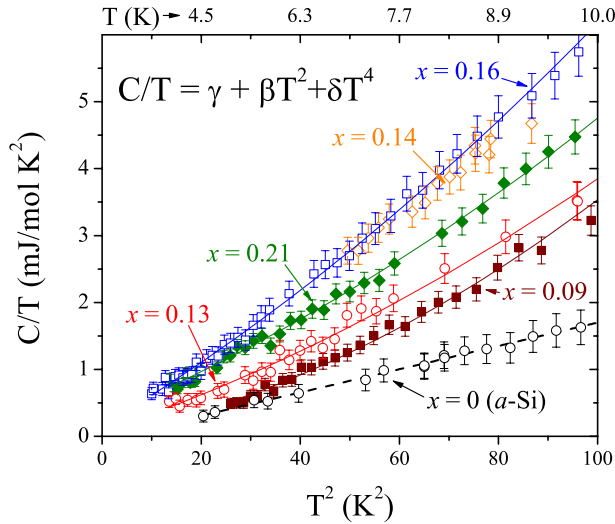
FIG. 1. (Color online) C/T vs T^2 for five a-Y$_x$Si$_{1-x}$ samples spanning the metal-insulator transition, as well as a-Si ($x=0$) (Ref. 25). The top axis labels indicate T, which is below 10 K here. Note that the data are not linear as predicted by the Debye T^3 law and that the $x=0.14$ and 0.16 samples have larger specific heat than the $x=0.21$ above ~6 K. The lines are the result of the fits to $C/T = \gamma + \beta T^2 + \delta T^4$.

and undoped amorphous-silicon thin film.[25] On this type of plot, a simple Debye specific heat is constant well below the Debye temperature, Θ_D, where $C \propto \beta T^3$, with a strong decrease at high T. A broad peak in C/T^3 is a feature nearly ubiquitous in amorphous solids and often seen in crystalline systems as well,[19] though typically smaller in magnitude than for amorphous systems. For the amorphous-silicon film, the peak shown is smaller than expected for an amorphous material, deviating less from the Debye model than does the
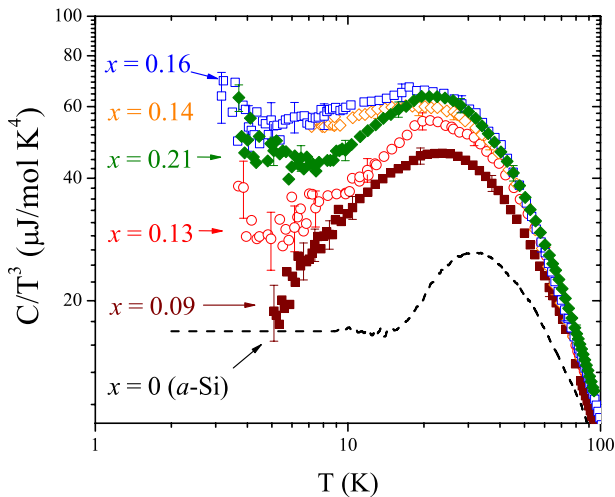
FIG. 2. (Color online) Data for the same a-Y$_x$Si$_{1-x}$ films measured to higher temperatures presented as C/T^3 vs T. Error bars are estimated assuming 2% error on both addenda and sample heat-capacity measurements and dominated by the background subtraction. a-Si is also shown for comparison (Ref. 25). All alloy samples show the significant "bump" associated with amorphous materials, and samples near the transition show an additional contribution.

crystalline phase.[25] Addition of even 9% Y causes a significant increase in C, which makes the peak closer to the expected size for a typical amorphous material.[31] For $x=0.21$, well on the metallic side of the transition, an electronic term is visible as a γ/T^2 upturn at low temperatures. It is obvious even with no further analysis that the $x=0.14$ and $x=0.16$ samples show qualitatively different behavior, with additional heat capacity below the C/T^3 peak.

IV. DISCUSSION

Before discussing our analysis in more detail, we note that our central conclusions are clear from the data by inspection. These are an additional contribution to C for compositions near the metal-insulator transition and somewhat different behavior of the electronic γ term than seen in other disordered systems measured to date. The goal of further analysis of our data is an attempt to investigate the contributions of vibrational and electronic excitations in order to probe the influence of the correlated-electron behavior that dominates near the metal-insulator transition. We believe that extending the range of our measurements well above 10 K clarifies the vibrational contributions and allows a different view of the electronic behavior near the transition.

The curvature of C/T vs T^2 apparent in Fig. 1 and reported by other authors already suggests a somewhat complicated vibrational spectrum that is not well described by a simple Debye (βT^3) model. When data only at these rather low temperatures are available, it is fairly common to introduce an additional term to Eq. (1) so that

$$\frac{C}{T} = \gamma + \beta T^2 + \delta T^4. \qquad (2)$$

As a first approach to the analysis of our data that allows relatively straightforward comparison to previous work, we performed fits of this type to the data shown in Fig. 1, limiting the fit to temperatures below 10 K (100 K^2). The solid lines shown in the figure are the resulting fits, and the parameters are shown in Fig. 3.

In many respects, the results of this fit agree with previous measurements of doped amorphous systems near the MIT. In particular, work on a-Mo$_x$Ge$_{1-x}$ reported similar trends in β [often related to a material's Debye temperature via the simple relation $\beta \approx 1944$ (J/mol K)/θ_D^3] and in δ.[13] The most notable departure from previous work on MIT systems in the strong disorder limit is the behavior of γ. Where other authors have reported values of γ near 0.51 mJ/mol K^2 that increase smoothly through the transition, the general trend of our results indicates γ near or within error bars of zero at or below the transition ($x_c \approx 0.135$) and increasing monotonically above the transition. Nonzero values of γ are on the same order of magnitude seen in systems such as Ti- and V-doped a-Si.[14–16] We note that the behavior of γ in crystalline Si is not simply monotonic with doping but drops sharply at a value slightly below the critical concentration.[5,6] Within our accuracy, the current results are similar to this behavior. More precise determination of γ for a-Y$_x$Si$_{1-x}$, which should be possible by measuring C to significantly lower temperatures, could indicate whether γ truly vanishes,
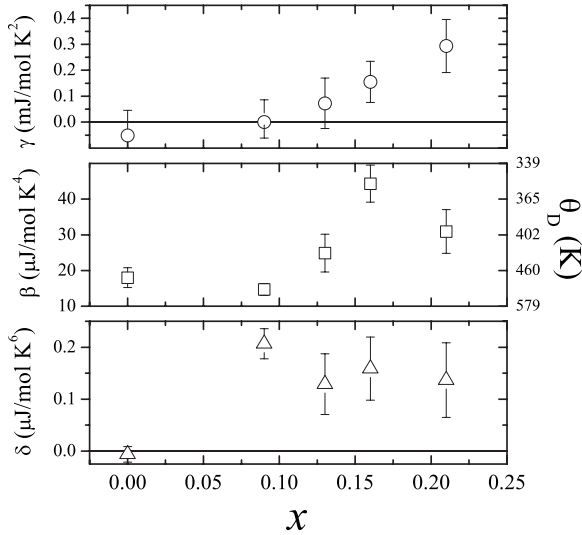
FIG. 3. Parameters from a fit of the data to Eq. (2) for temperatures only below 10 K. The MIT occurs near $x=0.14$ (Ref. 10). Results for $x=0.14$ are not shown as the data were not taken below 7 K.

or is simply finite but with much smaller values well below the transition.

The higher-temperature measurements made possible by the membrane microcalorimeters, as well as the comparison to similar data for amorphous silicon ($x=0$), allow a more detailed estimation of the vibrational excitations. In the filled skutterudite materials, heavy rare-earth atoms fill open cages in the skutterudite crystal structure. The motion of the cage-filling atom causes similar effects to our measurements of k and C of the doped a-Si: strongly decreasing the thermal conductivity and adding a contribution to C that can be modeled as one or more Einstein modes.[33–35] Therefore to better understand the addition of Y to the a-Si matrix, which leads to Y atoms in Si cages, we choose a model for specific heat that includes two Einstein modes. We fit our data from Fig. 2 to the expression,

$$\frac{C}{T^3} = \frac{C_{a-Si}}{T^3} + \frac{\gamma}{T^2} + \sum_{i=1}^{2} A_i \frac{\theta_{Ei}^2}{T^5} \frac{e^{(\theta_{Ei}/T)}}{(e^{(\theta_{Ei}/T)} - 1)^2}, \quad (3)$$

where γ is the electronic term, θ_{Ei} is the Einstein temperature, and A_i is the weight of each Einstein mode. As Eq. (3) shows, to fit our data we add two Einstein modes to the a-Si "background C," as well as allowing the simple metallic electronic term γ. This type of model assumes that the addition of dopants does not affect the matrix heat capacity and does not include complicated correlated-electron terms (in fact, it assumes an electronic system that can be described by the nearly-free-electron model). In materials such as the filled skutterudites, the electron-screening effects introduced by the doping can alter the vibrational character of the matrix;[33,36] a possibility we also consider below.

Figure 4 shows the result of the fit to Eq. (3) to the x =0.09, 0.16, and 0.21 samples (a similar fit for $x=0.13$ was performed but is not shown here; data for $x=0.14$ were not available below ~7 K, preventing a meaningful fit). Each
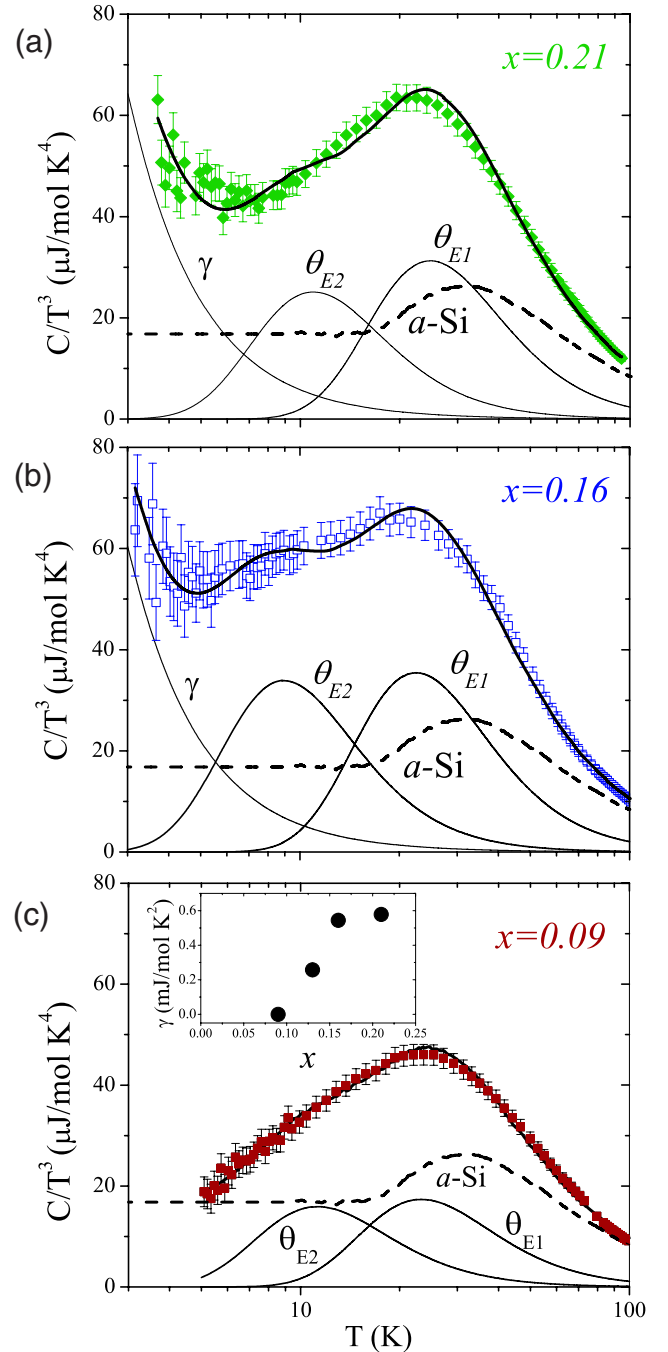
FIG. 4. (Color online) Fits of (a) $x=0.21$, (b) $x=0.16$, and (c) $x=0.09$ data to Eq. (3) shown with individual contributions from the a-Si matrix, the two Einstein modes, and for $x=0.21$ and $x=0.16$, the electronic contribution γ. The inset in (c) shows γ vs x that results from this fit. A similar fit of $x=0.13$ was performed and shows similar trends as $x=0.09$ and $x=0.13$ since data for $x=0.14$ were only taken above 7 K, no fit for this sample was possible. Data above 7 K are very similar to the results for $x=0.16$.

plot shows measured data and error bars, the resulting fit, and the contribution of each term in Eq. (3). Note that the fit of $x=0.09$ also suggests no significant γ term, in agreement with the simpler analysis presented earlier. Samples with $x>0.09$ do show finite γ with a similar dependence on x but somewhat larger values than given by the simpler fit. The
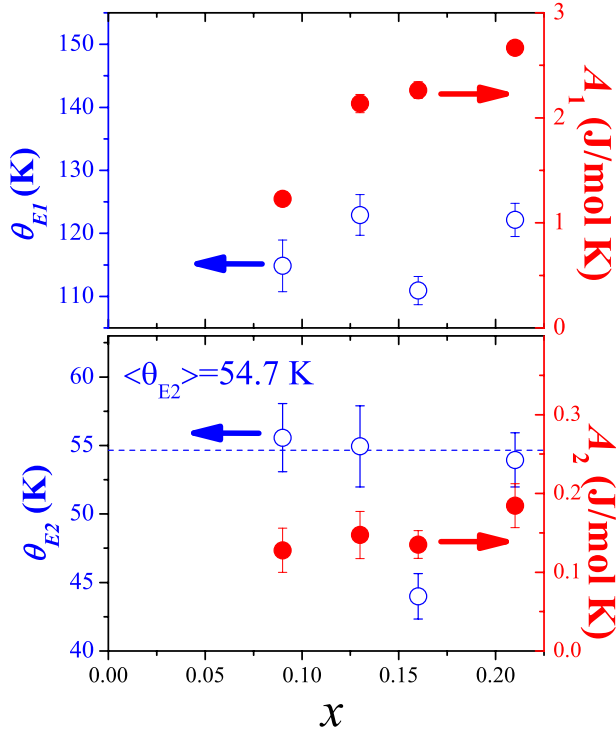
FIG. 5. (Color online) A_i (closed circles, right axes) and Θ_{Ei} (open circles, left axes) values determined from the fits to the data in Fig. 2. The dashed line in the lower frame indicates the weighted average of θ_{E2} excluding the $x=0.16$ value as discussed in the text.

results where γ is finite are still of comparable order of magnitude to previous measurements of similar systems.

The A_i and θ_{Ei} fit parameters as a function of x are shown in Fig. 5. These values summarize the VDOS information that can be extracted from our data. The error bars shown are the statistical errors from the fit. Films with $x=0.09$, 0.13, and 0.21 show generally similar trends, with values of θ_{E1} grouped near 120 K and θ_{E2} constant within error bars. The weight A_1 is very linear with increasing x and A_2 is reasonably linear (in both cases $A_i=0$ for $x=0$), suggesting that these features are directly associated with the addition of Y to a-Si, and could be interpreted as evidence of the localized "rattling" motion of the Y atom in its Si cage. For these three compositions, a weighted average gives $\theta_{E1}=121$ K and $\theta_{E2}=54.7$ K. The corresponding energies of the Einstein oscillators are $E_{E1}=10.4$ meV and $E_{E2}=4.7$ meV, simply determined from $E_{Ei}=k_B\theta_{Ei}$. E_{E1} is reasonably close to Meregalli and Parrinello's predicted 70 cm^{-1} (8.6 meV) feature, while E_{E2} is close to a feature at ~3–4 meV associated with the addition of Y to the matrix. However, the predicted pronounced dangling-bond peak at 22 meV is either absent shifted to a significantly lower energy (22 meV would represent $T_E=255$ K, which would be a peak on the C/T^3 plot at ~55 K) or too small to measure here. The absence of this peak would indicate that contrary to the local-density approximation (LDA) calculations, dangling bonds do not line the silicon cages that surround the dopant atom, in agreement with XAFS data on a-Gd$_x$Si$_{1-x}$.[30]

As is apparent from Figs. 4 and 5, though the $x=0.16$ sample can be fit to Eq. (3), the parameters do not follow the trend established for other compositions. To explain the enhanced C/T^3 below the peak using this model, the Einstein energies need to be significantly softened, particularly, the lower-energy mode. One interpretation of the enhanced C for the samples near the MIT on the metallic side is therefore a rather dramatic change in the vibrational spectrum. Such an effect could be explained by the reduction in effective spring constants by the increased electron screening as states become extended above the mobility edge. However, in this picture one would expect similarly softened vibrational states in the even more metallic $x=0.21$ sample rather than a return to the behavior seen below the transition. This suggests that a purely vibrational explanation of the additional specific heat may not be the correct view.

Another possible interpretation is that the clearly enhanced specific heat in $x=0.14$ and 0.16 samples is associated with the correlated-electron behavior near the metal-insulator transition, as seen in systems such as Si:P. However, a simple inspection of the C/T^3 vs T plot suggests that the behavior is quite different than the weak power-law term seen in the crystalline system. A rough estimate of the dependence of the enhanced specific heat observed here suggests that a contribution with much higher power of T between T^2 and T^3 develops in the regime below the C/T^3 peak (an additional term in $C\propto T^3$ would add a constant value simply shifting the curve in Fig. 2 upward). Such a large contribution from the Coulomb-gap-driven single occupation of electron states is unexpected but could be related to the much higher electron concentrations and strong disorder present in the amorphous system. Further measurements of additional samples near the transition over a broad range of temperature are needed to probe the physics of the enhanced specific heat.

V. CONCLUSION

In summary, we presented specific-heat measurements of a-Y$_x$Si$_{1-x}$ films spanning the metal-insulator transition from 3–100 K. Samples near the MIT show a clear additional contribution to specific heat. Within our accuracy $\gamma=0$ for the $x=0.09$ sample is within error bars of zero for the $x=0.13$ sample using the traditional analysis of the lowest-temperature data and is finite and smoothly varying for increasing x. A fit of the data to a model that adds two Einstein modes and an electronic term γ to the contribution of the a-Si matrix provide a reasonable explanation of results for samples with $x=0.09$, 0.13, and 0.21. The observed vibrational modes for these samples are similar to those predicted by the density-functional theory. However, a theoretically predicted mode at 22 meV associated with dangling bonds is not evident in our data suggesting that there are no dangling bonds, consistent with XAFS and ESR on similar alloys. This model fails to adequately explain the enhancement of specific heat seen in $x=0.14$ and 0.16 samples. Extending the range of this experiment to lower temperatures would be an

important addition to this work as it would allow more accurate determination of γ and investigation of tunneling states and excess modes as a function of metal content. In addition, measurements of samples with low x and use of other nonmagnetic dopants with different masses would offer the unique opportunity to study the electronic, magnetic, and vibrational degrees of freedom in amorphous semiconductor alloys in greater detail.

*barry.zink@du.edu

[1] P. A. Lee and T. V. Ramakrishnan, Rev. Mod. Phys. **57**, 287 (1985).

[2] P. W. Anderson, Phys. Rev. **109**, 1492 (1958).

[3] G. Hertel, D. J. Bishop, E. G. Spencer, J. M. Rowell, and R. C. Dynes, Phys. Rev. Lett. **50**, 743 (1983).

[4] M. Lee, Phys. Rev. Lett. **93**, 256401 (2004).

[5] M. Lakner, H. v. Löhneysen, A. Langenfeld, and P. Wölfle, Phys. Rev. B **50**, 17064 (1994).

[6] M. A. Paalanen, J. E. Graebner, R. N. Bhatt, and S. Sachdev, Phys. Rev. Lett. **61**, 597 (1988).

[7] A. Roy, M. Turner, and M. P. Sarachik, Phys. Rev. B **37**, 5522 (1988).

[8] A. Roy and M. P. Sarachik, Phys. Rev. B **37**, 5531 (1988).

[9] H. G. Schlager and H. von Lohneysen, Europhys. Lett. **40**, 661 (1997).

[10] E. Helgren, L. Zeng, K. Burch, D. Basov, and F. Hellman, Phys. Rev. B **73**, 155201 (2006).

[11] A. Möbius and M. Pollak, Phys. Rev. B **53**, 16197 (1996).

[12] A. Díaz-Sánchez, A. Möbius, M. Ortuño, A. Neklioudov, and M. Schreiber, Phys. Rev. B **62**, 8030 (2000).

[13] D. Mael, S. Yoshizumi, and T. H. Geballe, Phys. Rev. B **34**, 467 (1986).

[14] A. Rogatchev and U. Mizutani, Physica B **281-282**, 610 (2000).

[15] A. Y. Rogatchev, T. Takeuchi, and U. Mizutani, Phys. Rev. B **61**, 10010 (2000).

[16] U. Mizutani, T. Ishizuka, and T. Fukunaga, J. Phys.: Condens. Matter **9**, 5333 (1997).

[17] M. A. LaMadrid, W. Contrata, and J. M. Mochel, Phys. Rev. B **45**, 3870 (1992).

[18] R. C. Zeller and R. O. Pohl, Phys. Rev. B **4**, 2029 (1971).

[19] X. Liu and H. v. Lohneysen, Europhys. Lett. **33**, 617 (1996).

[20] P. W. Anderson, B. I. Halperin, and C. M. Varma, Philos. Mag. **25**, 1 (1972).

[21] W. A. Phillips, J. Low Temp. Phys. **7**, 351 (1972).

[22] X. Liu, B. E. White, Jr., R. O. Pohl, E. Iwanizcko, K. M. Jones, A. H. Mahan, B. N. Nelson, R. S. Crandall, and S. Veprek, Phys. Rev. Lett. **78**, 4418 (1997).

[23] R. O. Pohl, X. Liu, and E. Thompson, Rev. Mod. Phys. **74**, 991 (2002).

[24] J. L. Feldman, P. B. Allen, and S. R. Bickham, Phys. Rev. B **59**, 3551 (1999).

[25] B. L. Zink, R. Pietri, and F. Hellman, Phys. Rev. Lett. **96**, 055902 (2006).

[26] M. Mertig, G. Pompe, and E. Hegenbarth, Solid State Commun. **49**, 369 (1984).

[27] D. W. Denlinger, E. N. Abarra, K. Allen, P. W. Rooney, M. T. Messer, S. K. Watson, and F. Hellman, Rev. Sci. Instrum. **65**, 946 (1994).

[28] B. Revaz, B. L. Zink, and F. Hellman, Thermochim. Acta **432**, 158 (2005).

[29] V. Meregalli and M. Parrinello, Solid State Commun. **117**, 441 (2001).

[30] D. Haskel, J. W. Freeland, J. Cross, R. Winarski, M. Newville, and F. Hellman, Phys. Rev. B **67**, 115207 (2003).

[31] B. L. Zink, R. Islam, D. J. Smith, and F. Hellman, Phys. Rev. B **74**, 205209 (2006).

[32] E. Helgren, D. Queen, F. Hellman, L. Zeng, R. Islam, and D. J. Smith, J. Appl. Phys. **101**, 093712 (2007).

[33] J. L. Feldman, D. J. Singh, I. I. Mazin, D. Mandrus, and B. C. Sales, Phys. Rev. B **61**, R9209 (2000).

[34] R. P. Hermann, R. Jin, W. Schweika, F. Grandjean, D. Mandrus, B. C. Sales, and G. J. Long, Phys. Rev. Lett. **90**, 135505 (2003).

[35] V. Keppens, D. Mandrus, B. C. Sales, B. C. Chakoumakos, P. Dai, R. Coldea, M. B. Maple, D. A. Gajewski, E. J. Freeman, and S. Bennington, Nature (London) **395**, 876 (1998).

[36] J. L. Feldman, P. Dai, T. Enck, B. C. Sales, D. Mandrus, and D. J. Singh, Phys. Rev. B **73**, 014306 (2006).